

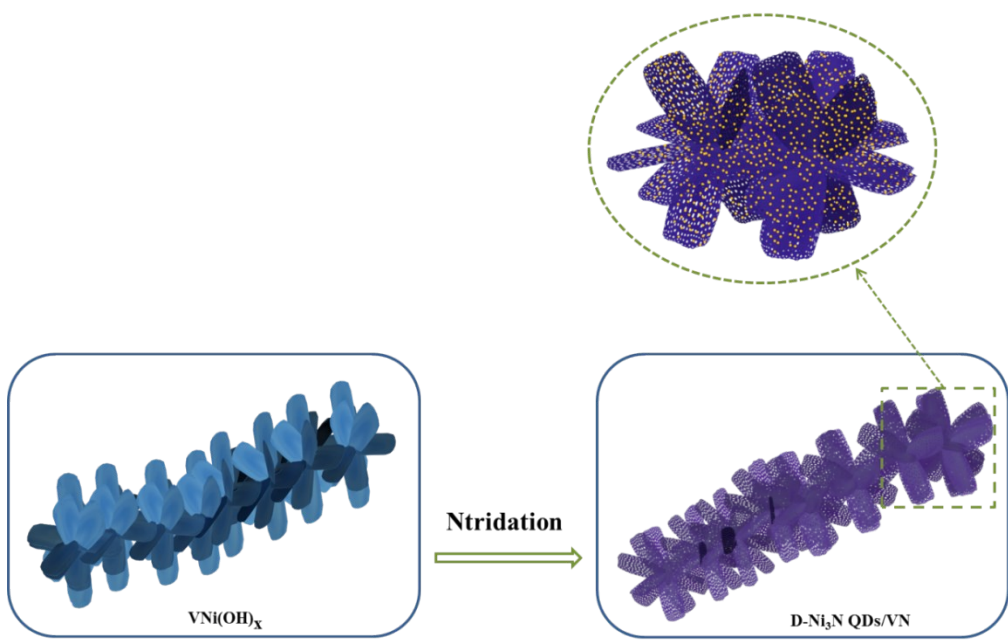
Supporting Information for

Distorted quantum dots enhancing efficient alkaline oxygen electrocatalysis

Xiaoyu Zhang¹, Weiwei Fu¹, Wu Tian¹, Jin Wan¹, Han Zhang^{2*} and Yu Wang^{1,2*}

¹The School of Chemistry and Chemical Engineering, State Key Laboratory of Power Transmission Equipment & System Security and New Technology, Chongqing University, 174 Shazheng Street, Shapingba District, Chongqing City 400044, PR China.

²The School of Electrical Engineering, Chongqing University, 174 Shazheng Street, Shapingba District, Chongqing City 400044, PR China.



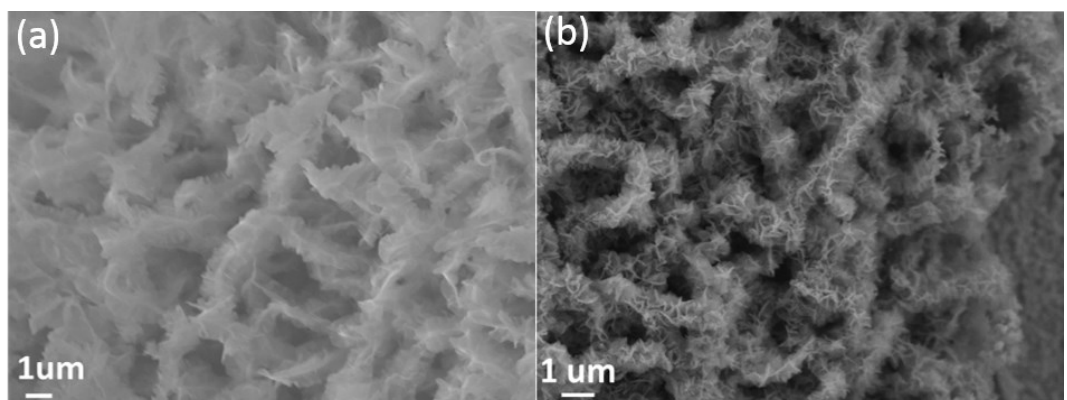


Fig. S1 (a, b) SEM images of widespread $\text{VNi}(\text{OH})_x$ and D- Ni_3N QDs/VN structures.

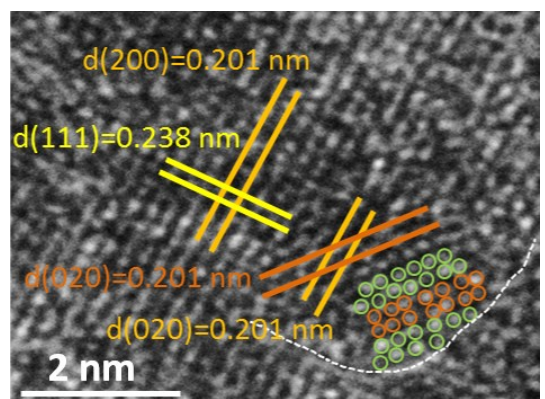


Fig. S2 High-magnification TEM image of D- Ni_3N QDs/VN.

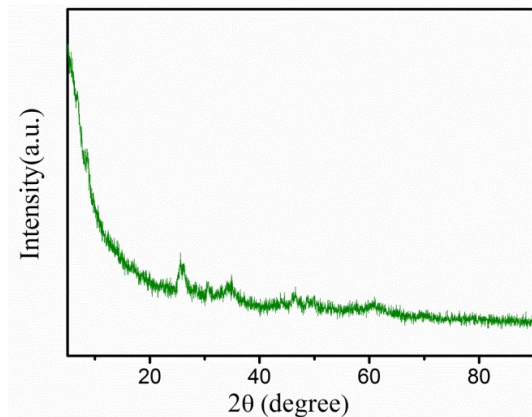


Fig. S3 XRD spectrum of VNi(OH)_x.

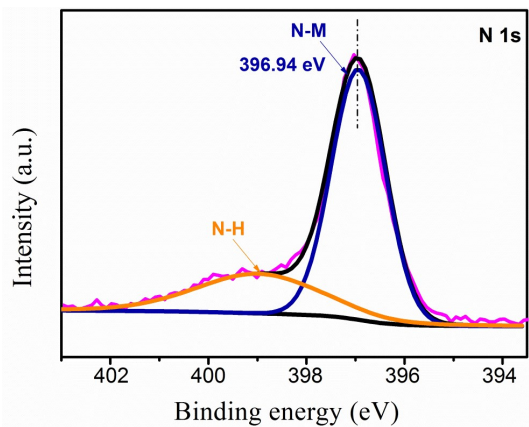


Fig. S4 High-resolution XPS spectrum of N1s.

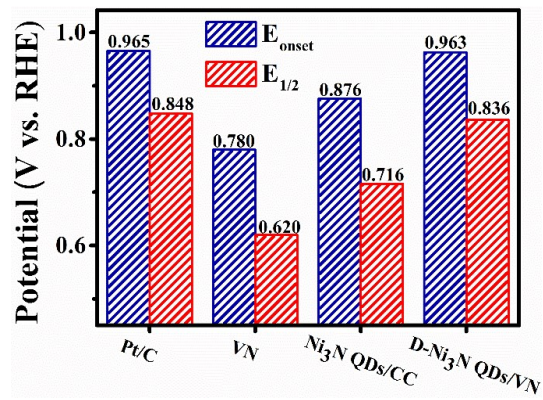


Fig. S5 Initial potentials and half-wave potentials of samples.

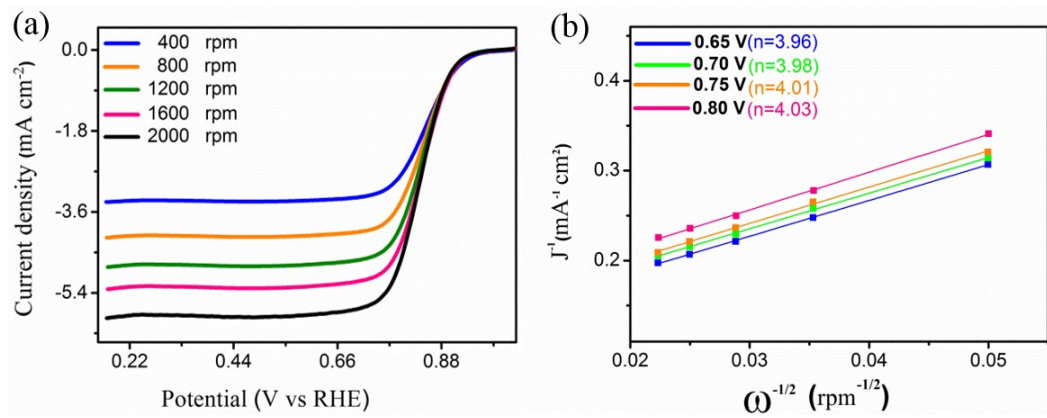


Fig. S6 (a) Polarization curves at different rotation rates of Pt/C. (b) Koutecky–Levich plots of Pt/C.

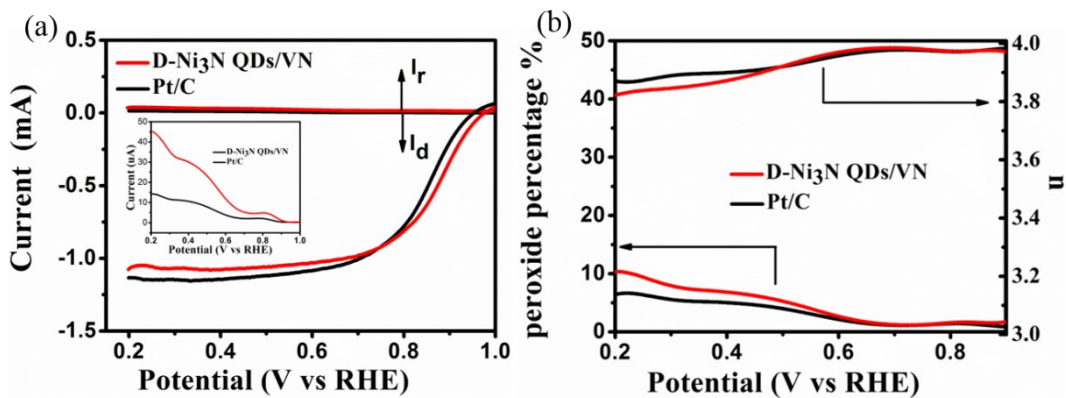


Fig. S7 (a) RRDE test on D-Ni₃N QDs/VN and Pt/C in O-saturated 0.1 M KOH solution, respectively. (b) Corresponding peroxide percentage and electron transfer number of ORR. The H₂O₂ yield of D-Ni₃N QDs/VN is 1.2-10%, slightly higher than Pt/C (1-6.8%) in the same range of ORR test. The electron transfer number (*n*) of ORR on D-Ni₃N QDs/VN is 3.83-3.98, whereas the *n* value of Pt/C is 3.86-3.98. The result demonstrates a 4-electron oxygen reduction pathway on the surface of D-Ni₃N QDs/VN.¹ We use the following equation to calculate the electron transfer number (*n*) and the peroxide percentage.²

$$n = 4 * \frac{I_d}{I_d + I_r/N}$$

$$H_2O_2\% = 200 * \frac{I_r/N}{I_d + I_r/N}$$

Where I_d is the disk current, I_r is the ring current, and N is the collection efficiency (0.37) of the ring electrode.³

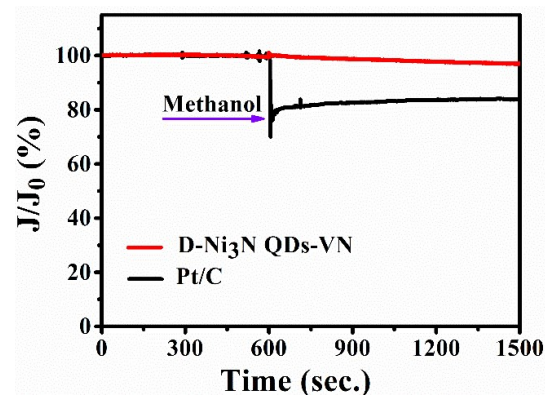


Fig. S8 Methanol tolerance test of D- Ni_3N QDs/VN and Pt/C.

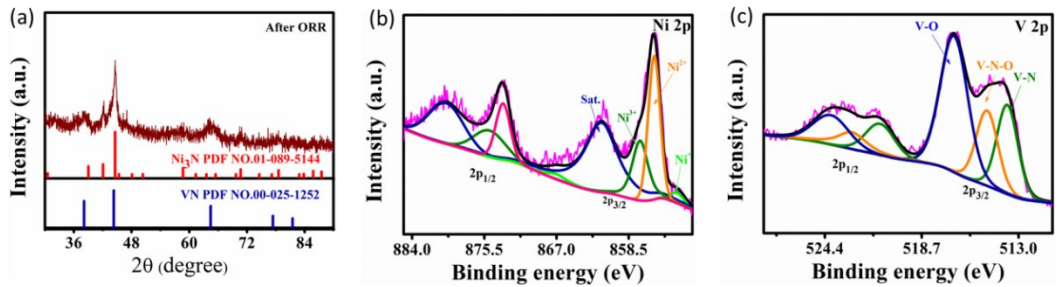


Fig. S9 (a) The XRD spectrum of D-Ni₃N QDs/VN after ORR test. (b, c) High-resolution XPS spectra of Ni 2p and V 2p for post-test D-Ni₃N QDs/VN.

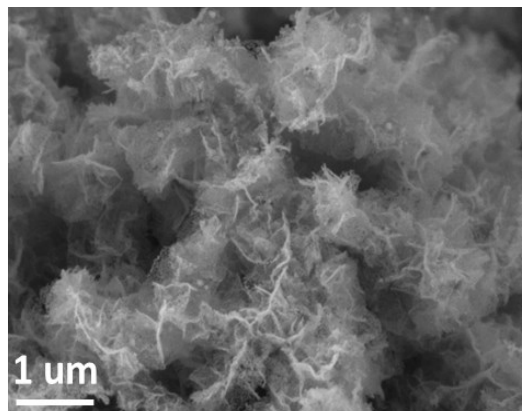


Fig. S10 SEM image of D-Ni₃N QDs/VN after ORR.

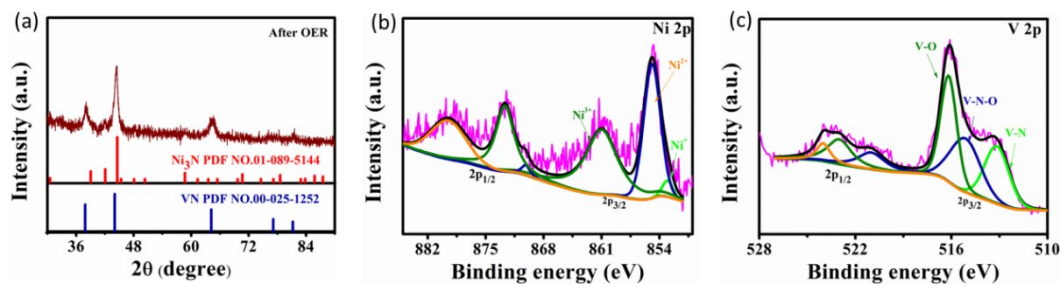


Fig. S11 (a) The XRD spectrum of D-Ni₃N QDs/VN after OER test. (b, c) High-resolution XPS spectra of Ni 2p and V 2p for post-test D-Ni₃N QDs/VN.

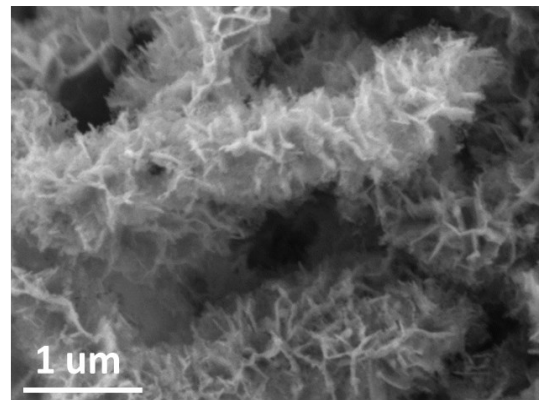


Fig. S12 SEM image of D-Ni₃N QDs/VN after OER.

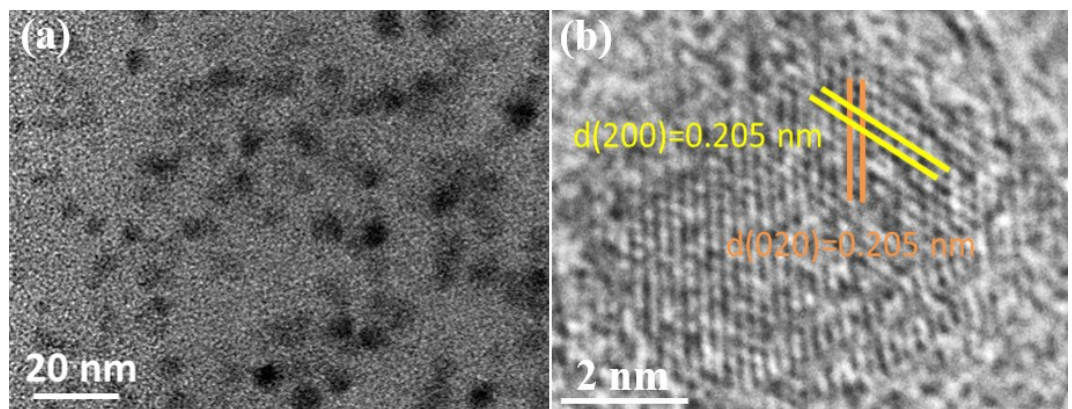


Fig. S13 (a) TEM image of widespread Ni_3N QDs/CC, (b) High-magnification TEM image of Ni_3N QDs/CC.

Table S1. Comparison of the catalytic activity of D-Ni₃N QDs/VN to the reported transition-metal-based ORR catalysts

| No. | catalysts | electrolyte | E ₀ vsRHE (V) | E _{1/2} (V) | b (mV/dec) | Ref. |
|-----|--|-------------|--------------------------|----------------------|------------|--|
| 1 | Ni/N-CNCs | 0.1 M KOH | 0.925 | 0.775 | - | Adv. Mater. 2017, 29, 1605083 |
| 2 | V _{0.95} Co _{0.05} N MFs | 0.1 M KOH | 0.903 | 0.802 | - | ACS Appl. Mater. Interfaces 2018, 10, 11604–11612 |
| 3 | Ni ₃ Fe/N-C | 0.1 M KOH | - | 0.810 | 79 | J. Electroanal. Chem. 851 (2019) 113418 |
| 4 | Co/Ni-N-C | 0.1 M KOH | 0.930 | 0.840 | - | Appl. Catal. B 240 (2019) 112–121 |
| 5 | CSV10 | 0.1 M KOH | 0.797 | 0.737 | 120 | Carbon 144 (2019) 289e300 |
| 6 | Co-NiMoN | 0.1 M KOH | 0.890 | 0.730 | - | ACS Appl. Mater. Interfaces 2019, 11, 27751-27759 |
| 7 | FeNi ₃ N/NG | 0.1 M KOH | 0.880 | 0.790 | 83 | J. Mater. Chem. A, 2019, 7, 1083 |
| 8 | FeNC-900 | 0.1 M KOH | 0.959 | 0.837 | 86.2 | Nanoscale 2019, 11, 19506-19511 |
| 9 | W ₂ N/WC | 0.1 M KOH | 0.930 | 0.810 | - | Adv. Mater. 2020, 32, 1905679 |
| 10 | D-Ni ₃ N QDs/VN | 0.1 M KOH | 0.963 | 0.837 | 81 | This work |

Table S2. Comparison of the catalytic activity of D-Ni₃N QDs/VN to the reported transition-metal-based OER catalysts

| No. | catalysts | electrolyte | η (mV) | b (mV/dec) | Ref. |
|-----|-----------------------------------|-------------|---------------------|------------|--|
| 1 | Ni ₃ FeN | 0.1 M KOH | $\eta_{j=10} = 355$ | 70 | Nano Energy 39 (2017) 77–85 |
| 2 | Ni ₃ N/NC | 1.0 M KOH | $\eta_{j=10} = 310$ | - | Chem. Commun., 2017, 53, 9566–9569 |
| 3 | Ni ₃ N/NC holey sheets | 1.0 M KOH | $\eta_{j=10} = 260$ | 51 | ACS Appl. Energy Mater. 2018, 1, 6774–6780 |
| 4 | Ni ₃ Fe/N-C | 1.0 M KOH | $\eta_{j=10} = 310$ | 58 | J. Electroanal. Chem. 851 (2019) 113418 |
| 5 | NiCo ₂ N | 1.0 M KOH | $\eta_{j=10} = 289$ | 56 | Adv. Mater. Interfaces 2019, 6, 1900960 |
| 6 | NB-HO | 1.0 M KOH | $\eta_{j=10} = 247$ | 79 | J. Mater. Chem. A, 2019, 7, 22063 |
| 7 | NiMoN-400 NRs | 1.0 M KOH | $\eta_{j=10} = 294$ | 73 | ACS Appl. Mater. Interfaces 2019, 11, 27751–27759 |
| 8 | N-NiVFeP/NFF | 1.0 M KOH | $\eta_{j=10} = 229$ | 72.6 | Appl. Catal. B 268 (2020) 118440 |
| 9 | W ₂ N/WC | 1.0 M KOH | $\eta_{j=10} = 320$ | 94.5 | Adv. Mater. 2020, 32, 1905679 |
| 10 | D-Ni ₃ N QDs/VN | 0.1 M KOH | $\eta_{j=10} = 226$ | 54 | This work |

Reference

1. X. Han, W. Zhang, X. Ma, C. Zhong, N. Zhao, W. Hu and Y. Deng, *Advanced materials*, 2019, **31**, e1808281.
2. S. Wang, L. Zhang, Z. Xia, A. Roy, D. W. Chang, J. B. Baek and L. Dai, *Angewandte Chemie*, 2012, **51**, 4209-4212.
3. C. Du, P. Li, F. Yang, G. Cheng, S. Chen and W. Luo, *ACS applied materials & interfaces*, 2018, **10**, 753-761.